Appl. Phys. B 66, 539–542 (1998)

Applied Physics B
Lasers
and Optics


# High optical-to-optical efficiency of LD pumped cw Nd:YAG laser under pumping distribution control

**J. Song, A.P. Liu, D.Y. Shen, K. Ueda**

Institute for Laser Science, University of Electro-Communications, 1-5-1 Chofugaoka, Chofu, Tokyo 182, Japan
(Fax: +81-424/85-8960, E-mail: song@ils.uec.ac.jp)

Received: 10 June 1997

**Abstract.** The input and output characteristics of an LD pumped Nd:YAG laser of cw $TEM_{00}$ operation have been investigated under different pump light distributions that have been formed by a virtual-point-source pumping system. Compared with a central uniform distribution, a centrally depressed distribution is found to have a lower thermal lensing effect and a higher optical-to-optical efficiency for operations performed using the same resonator parameters or within a similar stable range, and the improvement in optical-to-optical efficiency is explained as a result of a reduction in thermally induced aberrations.

**PACS:** 42.60; 42.55

Laser-diode (LD) pumped all-solid-state lasers operating at high cw levels have attracted a good deal of attention in recent years in the fields of gravity-wave detection, universal communication, materials processing and nonlinear frequency conversion. This is because such lasers have the advantages of being compact, efficient and scalable, and having a long lifetime.

Although the LD end-pumped lasers are more efficient in $TEM_{00}$ mode operations [1], they are limited to low power levels because of the relatively big thermal effect on the small pumping area of the laser material. For pump power more than 100 W, side-pumped configurations are generally adopted, and transversal multi-mode operations have been used up to 320 W. $TEM_{00}$ mode operations up to 80 W have been reported [2, 3]. The obstacles that limit the power-scaling ability of $TEM_{00}$ operation are mainly those arising from thermally induced effects, which include thermal lensing, thermal aberration and thermal stress-induced birefringence effects. For the thermal lensing effect, the resonator parameter becomes power-dependent and the stable range (or dynamic range) becomes narrow. Although theoretically the stable range of the resonator can be designed up to the maximum available power, in practice the other two thermal effects become so big that $TEM_{00}$ operation actually becomes impossible when the pump power is very high [2, 4, 5].

Methods of solving these problems are generally concentrated on careful resonator design, where a more stable operation configuration is chosen [6], and two laser rods with aspherical surfaces are used to correct birefringence spherical aberration [5]. In our work described here, we investigated $TEM_{00}$ operational characteristics using a central depressed pump light distribution formed by a virtual-point pumping source. Compared with the results from a centrally uniform distribution, output power increases of about 40% and 10% respectively were achieved for operations performed with fixed resonator parameters and with variable parameters that let the laser lase at its maximum input power. The corresponding optical-to-optical efficiency was increased in the range 9.3–12.6%. The thermal lensing effect was also considered, and estimated to have decreased by about 10%.

The improvement in optical-to-optical efficiency is explained as a result of a reduction in thermally induced aberrations. Thus, the total thermally induced effect in the centrally depressed pump light distribution is reduced.

## 1 Experimental method

The pumping geometry we used to form the different pump light distributions is called virtual point source (VPS), which has been described previously [7, 8]. A schematic diagram of the VPS is shown in Fig. 1. We used 32 sets of ten-watt laser diodes (807 nm wavelength) made by McDonnell Douglas, and these formed a symmetrical ring-shaped pumping source so as to get better angular uniformity. The outputs of the diodes were focused into a point (or line) at the rod axis by 32 sets of optics, each comprising a cylindrical lens and a high reflectivity (HR) spherical mirror. The axial illumination was completed by a coaxial cylinder with Ag-coated side surface and Au-coated end surfaces, which, in all, acting like a huge double-cladding fiber. The point of focus, acting as a virtual point source, was imaged and re-imaged along the rod axis and reflected by the end surface, so that after multiple passes the whole of the laser rod was illuminated.

To ensure axial uniformity, the laser rod had to be optically thin to let the pump light be absorbed after multiple

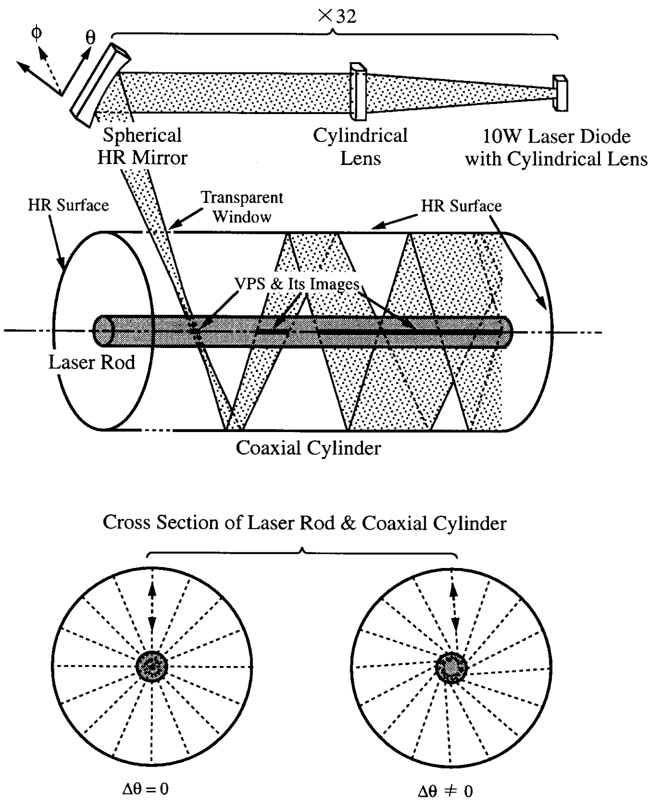


**Fig. 1.** Schematic diagram of the virtual-point pumping source (VPS). The change in pump light distribution is illustrated in the *lower part* of the figure, and is achieved by rotating the spherical mirror along its $\theta$ axial

passes instead of a single pass. In our experiment, we used a Nd:YAG rod 104 mm in length and 4 mm in diameter, with a $Nd^{3+}$ doping concentration of 0.6 at.%. The end faces of the rod were flat and antireflection-coated at a wavelength of 1064 nm. The laser cavity was constructed by a HR mirror and an output coupling mirror with 20% transmission. The distance from the center of the rod to the HR mirror ($L_2$ in the diagram) was fixed at 75 cm, while the distance to the coupling mirror, $L_1$, was either fixed or varied for operations using different pump light distributions. Both mirrors were flat, and the stable range was chosen to be insensitive to thermal length fluctuations and to misalignment [6].

By rotating the spherical mirrors along their $\theta$ axes, the pump light distributions were able to be changed from a centrally intense distribution ($\Delta\theta = 0$) to centrally uniform or centrally depressed ones ($\Delta\theta \neq 0$). In practice, we divided the 32 LDs into four groups called LD-A, B, C and D, and we rotated each group into a different angle to achieve a more flexible pump light distribution. We set up our desired pump light distributions based on the calculated results from a ray-tracing program. The centrally uniform pump light distribution (see Fig. 2a) was formed by setting the rotation angles $\Delta\theta$ of LD-A, B, C and D to be 0.0°, 0.4°, 0.2° and 0.4° respectively. For the centrally depressed distribution (see Fig. 2b), these angles were changed to 0.0°, 0.4°, 0.3° and 0.4° respectively, i.e. the rotation angle for set LD-C alone was altered.

## 2 Results and discussion

The thermal lensing effect was modeled as an equivalent thin lens at the center of the rod, with an effective focal length of $f_T$ [8] and the cavity parameters $L_1$ and $L_2$ in the resonator's theoretical calculation changed to $L_1^*$ and $L_2^*$, as determined from the two principal planes [6]. According to the theoretical analysis by Magni [6] as applied to the simple case in our experiment where the two cavity mirrors are flat, the width of the stable range and the minimum mode size $\omega_{f_0}$ at the thermal lens are only dependent upon the value of $L_2^*$, which remained the same in our experiment. The dependence of the mode size $\omega_f$ at the thermal lens, and mode sizes heat $\omega_a$ and $\omega_b$ at the two ends of the rod, as a function of the dioptric power is shown in Fig. 3, with $L_1^* = 32.7$ cm and 23.0 cm respectively.

With $L_1^*$ fixed at 32.7 cm, the input and output characteristics using two pump light distributions under $TEM_{00}$ operation are shown in Fig. 4. The maximum output power of the centrally uniform distribution (see $a_1$ in Fig. 4) is 30 W with an input power of about 212 W, and the corresponding optical-to-optical efficiency is about 14.1%. For the centrally depressed distribution (see $b_1$ in Fig. 4), the maximum output power is increased to 36 W with input power of around 225 W, and the optical-to-optical efficiency is then about 16.0%.

Usually, the dioptric power (the reciprocal of $f_T$) is proportional to the pump power $P_{in}$, so we can write

$$1/f_T = A_T P_{in} , \quad (1)$$

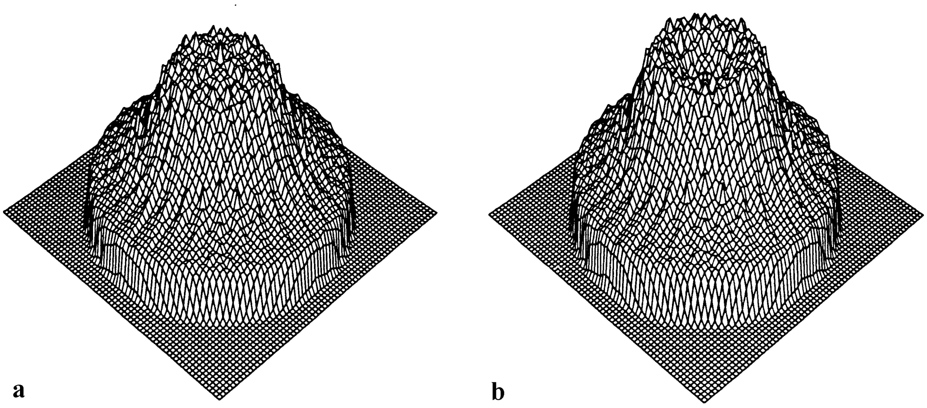


**Fig. 2a,b.** The pump light distribution obtained from a ray-tracing calculation from a Nd:YAG rod 4 mm in diameter and with a doping concentration of 0.6 at.%. **a** The centrally uniform pump light distribution; **b** the centrally depressed pump light distribution

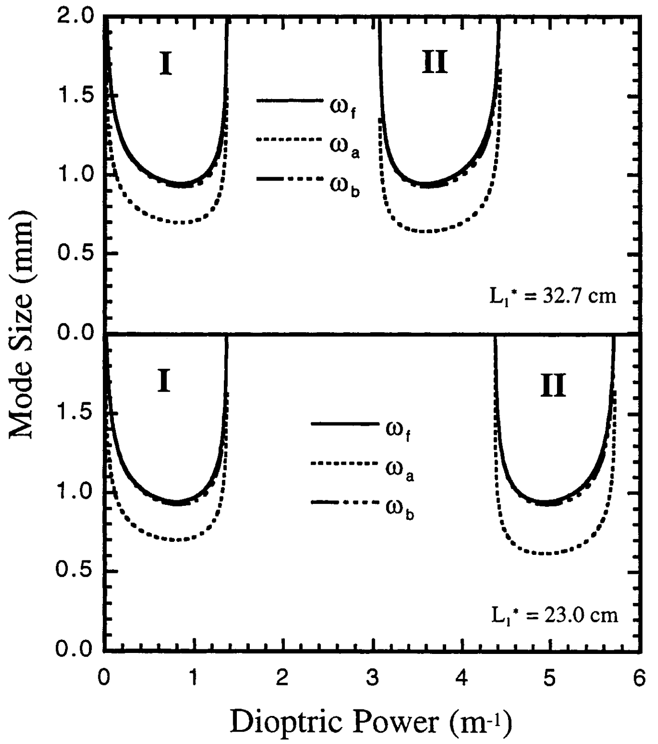


**Fig. 3.** Calculated mode sizes in the center of the laser rod ($\omega_f$) and on its two ends ($\omega_a$, $\omega_b$) as a function of the dioptric power for $L_1^* = 32.7$ cm (*top*) and $L_1^* = 23.0$ cm (*bottom*)

where $A_T$ is the coefficient (to be determined) that describes the extent of the thermal lensing effect. By application of (1) to the minimum and the maximum points of the stable ranges, the values of $A_T$ can be estimated by combining the results shown in Figs. 3 and 4. The values of $f_T$ determined from Fig. 3 are the same for the same $L_1^*$, while the values of $P_{in}$ achieved from Fig. 4 are different for different pump distributions. Results estimated from Fig. 4 show that the thermal lensing effect of the centrally depressed distribution is decreased by about 10% at the two critical points compared with that of the centrally uniform distribution.

This result was confirmed by direct measurement of the effective focal length with a He–Ne laser. The collimated output of 632.8 nm was passed through the YAG rod and the beam waist was determined by a knife edge. The measured focal length as a function of the pump power is shown in Fig. 5, the decrease of the thermal lensing effect being about 6%. The two sets of estimated values obtained from the input–output characteristics of Fig. 4 are also shown in Fig. 5 for comparison.

There are two possible reasons for the increase of output power when using the centrally depressed pump light distribution. One is a reduction in thermal lensing effect, which causes the shifting of the stable range to the higher side of the pump power, and thus a higher output can be achieved. The other is a reduction in aberration and/or birefringence, which reduces the related loss.

Since the shifting of the stable range can also be achieved by changing the distance of $L_1^*$, and the mode size was found to remain almost unchanged for different $L_1^*$ (as seen from Fig. 3), we performed further investigations using different $L_1^*$ for the same centrally uniform distribution. The input and output characteristics found are shown in Fig. 6 as $a_2$ and $a_3$, for $L_1^*$ set at 25.7 cm and 23.0 cm respectively. For $a_2$, the maximum output power is 38 W with 260 W pump power, and the optical-to-optical efficiency is 14.6%. For $a_3$, the maximum output power is 42 W with 291 W pump power, and the efficiency is 14.4%. By comparing the result $a_1$ in Fig. 4, we can deduce that the maximum output power increases when the stable range is shifted to the higher power side, but the optical-to-optical efficiency remains almost the same.

Furthermore, we performed the same operation for the centrally depressed distribution, whose maximum stable point was designed around the maximum pump power of 291 W, as performed by $a_2$. The result is also shown in Fig. 6

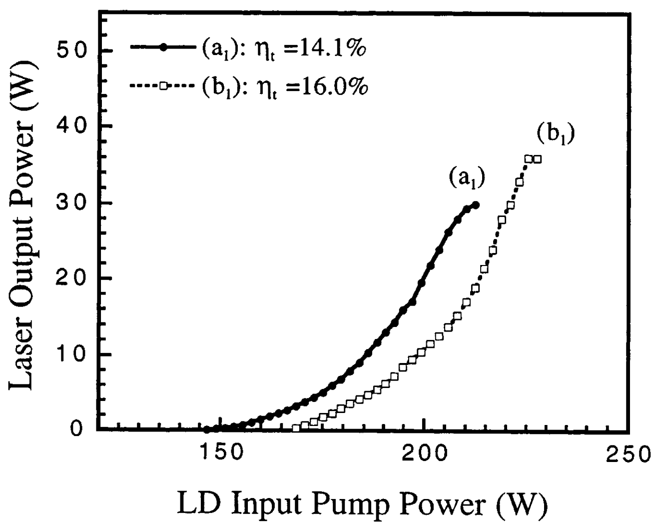


**Fig. 4a,b.** The input and output characteristics $a_1$ and $b_1$ of the two pump light distributions **a** and **b**, respectively, under $TEM_{00}$ operation with $L_1^* = 32.7$ cm

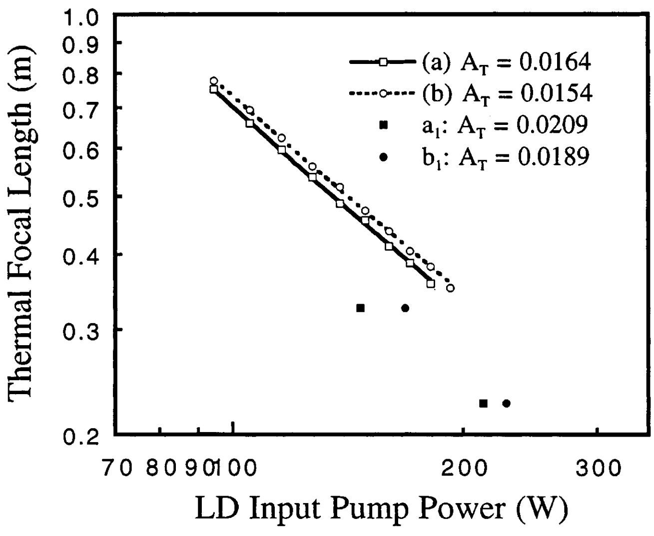


**Fig. 5a,b.** Effective focal length of our laser rod as a function of pump power as measured by a probe He–Ne laser (*outline symbol*) and the estimated values obtained from resonator theory (*solid symbol*). The $A_T$ values are calculated by fitting or direct use of (1). The results of distributions **a** and **b** are distinguished by the *squares* and *circles*

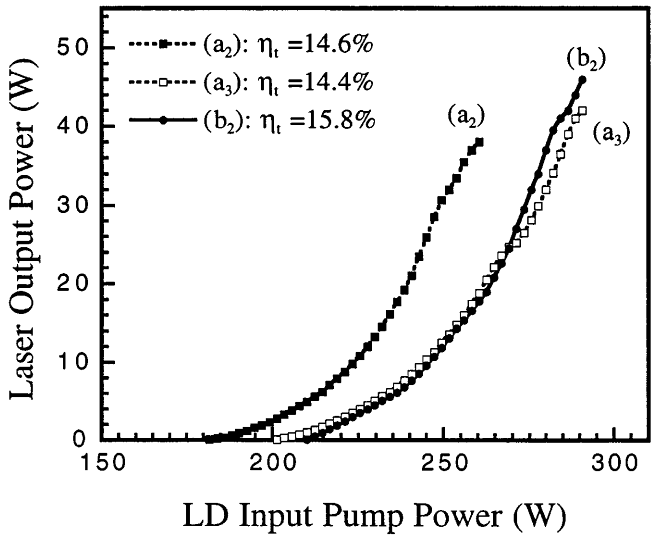


**Fig. 6a,b.** The input and output characteristics $\{a_2, a_3\}$ and $b_2$ of the two pump light distributions **a** and **b** respectively, under $TEM_{00}$ operation with their maximum stable points designed at the maximum pump power point

as $b_2$, with $L_1^* = 24.7$ cm in this case. About 15.8% optical-to-optical efficiency was obtained, with a maximum output power of 46 W. Combining the results of Fig. 4 and Fig. 6, we can see that by using the centrally depressed pumping distribution, the optical-to-optical efficiency is increased in the range 9.3–12.6% at different pump-power ranges. This shows that, besides a reduction in thermal lensing effect achieved by using a centrally depressed pumping distribution, the aberration and/or birefringence should also be reduced and thus provide an increase in optical-to-optical efficiency.

The reason that the centrally depressed distribution gives a more efficient result comes from the temperature-dependence of the thermal conductivity. Because of this dependence, the thermal aberration, which is generally caused by inhomogeneous illumination, can still occur even for a homogeneous illumination. Analyses performed by N. Hodgson and H. Weber [4] show that by choosing a properly shaped pump distribution, which is similar to our centrally depressed distribution, the aberration can be compensated for at a fixed pump power. We also performed a similar operation using a more depressed distribution, but in this case the efficiency at maximum pump power was found to decrease, which suggests over-compensation on this occasion.

## 3 Conclusion

In summary, we have demonstrated a useful way to reduce the thermally induced effect of thermal lensing and aberration, and we have therefore improved the output power and optical-to-optical efficiency of the laser. This has been accomplished by using a centrally depressed pump light distribution. The efficiency was found to increase in the range 9.3–12.6% as compared with the results from a centrally uniform distribution, and the thermal lensing effect decreased by about 10%.

## References

1. S.C. Tidwell, J.F. Seamans, M.S. Bowers, A.K. Cousins: IEEE J. Quantum Electron. **28**, 997 (1992)
2. D. Golla, M. Bode, S. Knoke, W. Schöne, A. Tünnermann: Opt. Lett. **21**, 210 (1996)
3. D. Golla, S. Knoke, M. Bode, W. Schöne, A. Tünnermann, H. Welling: Proc. SPIE **2700**, 314 (1996)
4. N. Hodgson, H. Weber: IEEE J. Quantum Electron. **29**, 2497 (1993)
5. S.C. Tidwell, J.F. Seamans, M.S. Bowers: Opt. Lett. **18**, 116 (1993)
6. V. Magni: Appl. Opt. **25**, 107 (1986)
7. N. Uehara, K. Nakahara, K. Ueda: Opt. Lett. **20**, 1707 (1995)
8. J. Song, A.P. Liu, K. Okino, K. Ueda: Appl. Opt. **36**, 8051 (1997)